Contents lists available at ScienceDirect

Deep-Sea Research II

journal homepage: www.elsevier.com/locate/dsr2

The influence of long tides on ecosystem dynamics in the Barents Sea

Harald Yndestad *

Aalesund University College, N-6025 Aalesund, Norway

ABSTRACT

The Barents Sea ecosystem has been associated with large biomass fluctuations. If there is a hidden deterministic process behind the Barents Sea ecosystem, we may forecast the biomass in order to control it. This presentation concludes, for the first time, investigations of a long data series from North Atlantic water and the Barents Sea ecosystem. The analysis is based on a wavelet spectrum analysis from the data series of annual mean Atlantic sea level, North Atlantic water temperature, the Kola section water temperature, and species from the Barents Sea ecosystem.

The investigation has identified dominant fluctuations correlated with the 9.3-yr phase tide, the 18.6-yr amplitude tide, and a 74-yr superharmonic cycle in the North Atlantic water, Barents Sea water, and Arctic data series. The correlation between the tidal cycles and dominant Barents Sea ecosystem cycles is estimated to be $R = 0.6$ or better. The long-term mean fluctuations correlate with the 74-yr superharmonic cycle. The wavelets analysis shows that the long-term 74-yr cycle may introduce a phase reversal in the identified 18-yr periods of temperature and salinity. The present analysis suggests that forced vertical and horizontal nodal tides influence the ocean's thermohaline circulation, and that they behave as a coupled non-linear oscillation system.

The Barents Sea ecosystem analysis shows that the biomass life cycle and the long-term fluctuations correlate better than $R = 0.5$ to the lunar nodal tide spectrum. Barents Sea capelin has a life cycle related to a third harmonic of the 9.3-yr tide. The life cycles of shrimp, cod, herring, and haddock are related to a third harmonic of the 18.6-yr tide. Biomass growth was synchronized to the lunar nodal tide. The biomass growth of zooplankton and shrimp correlates with the current aspect of lunar nodal tidal inflow to the Barents Sea. The long-term biomass fluctuation of cod and herring is correlated with a cycle period of about $3 \times 18.6 = 55.8$ yr. This analysis suggests that we may understand the Barents Sea ecosystem dynamic as a free-coupled oscillating system to the forced lunar nodal tides. This free-coupled oscillating system has a resonance related to the oscillating long tides and the third harmonic and superharmonic cycles.

1. Introduction

The idea of a hidden process that influences the biomass ecosystem originated in the early period of marine science. The motive has been to develop better long-term predictions. If there is a hidden deterministic process, we may forecast the biomass in order to control it. If there is none, we may explain past biomass dynamics only as a random chain of events. Early ideas regarding this hidden process are related to sun spots (Ljungman, 1879; Lindquist, 2002), climate change, and long tides. The British astronomer Edmond Halley (1656–1742) is probably the first to publish a paper on the influence of climate on biomass in the North Sea. In the paper *Atlas matitimus et commercialis* of 1728, he described the theory of a fluctuating herring stock between the Arctic Ocean and the North Sea that was controlled by climate

conditions (Wegner, 1996). During the last 100 yr, the relation between climate conditions and Barents Sea biomass fluctuations was described by Helland-Hansen and Nansen (1909), Sætersdal and Loeng (1987), Ellertsen et al. (1989), Nakken (1994), Hylen (2002), Godø (2003), and many others. The climate and sea temperature have, however, their own complex pattern. When the climate variability is unknown, the possibility of a hidden deterministic biomass process is unknown.

Long tides are a possible source of the hidden deterministic process that may influence climate and biomass fluctuations. George Darwin recorded fluctuations of the sea level at Bombay and was the first to draw attention to how the 18.6-yr lunar nodal cycle introduced a long-term tide as well as geological changes (Darwin, 1880). Otto Pettersson (1905, 1915, 1930) investigated the herring catch records from Bohuslen in Sweden and found a relationship between the sea temperature, tide periods, and herring periods. From this study, he saw a relation between the long-term waves and extreme climate events and biomass fluctuations. A number of Russian scientists expounded on the

* Tel.: +47 70 16 12 00; fax: +47 70 16 13 00.
  E-mail address: Harald.Yndestad@hials.no

ideas from Otto Pettersson in the 1960s. The results were summarized by Maksimov and Smirnov (1964, 1965, 1967), Maksimov and Sleptsov-Shevlevich (1970) and explained as a standing wave and a standing "astronomical" current in the North Atlantic and Barents Sea, which influence the climate. The 18.6-yr tidal water temperature in the North Atlantic was expressed by the equation $T_{18.6}(t) = 0.24\,°\mathrm{C}\sin(19.35°t+80°)$, where $T_{18.6}(t)$ has a maximum in 1950 and a minimum in 1959.

From the 1960s, new computers and spectrum analysis methods were introduced to identify periodic cycles in long data series. Currie et al. (1993) identified the 18.6-yr lunar nodal cycle period in climate, agriculture, rainfall, vine harvest, and the biomass in the sea. Wyatt et al. (1994) published a spectrum analysis of Lofoten cod records that showed an 18.6-yr cycle in landings of Northeast Arctic cod. Mazzarella and Palumbo (1994) identified an 18.6-yr cycle in atmospheric oscillations. Royer (1993) and Keeling and Whorf (1997) estimated an 18.6-yr tide in the Atlantic Ocean. The spectrum analysis method had, however, a limited ability to analyze data series from nature. The time-variant property limits the possibility of estimating the periodic cycle and results in the loss of phase and timing events.

Introduction of the wavelet spectrum analysis method opened the possibility to study each cycle period and phase in the data series. By this new analysis approach, a lunar nodal cycle spectrum was identified in data series of zooplankton, shrimp, capelin, herring, and haddock in the Barents Sea ecosystem (Yndestad and Stene, 2002; Yndestad, 2003a, b). The wavelet analysis confirmed the hypothesis that a hidden deterministic process influenced the biomass ecosystem. At the same time, a phase reversal related to the lunar nodal tide in the Kola section temperature data series was identified. The phase reversal introduced limited long-term prediction and a new understanding of long-term dynamics. A number oceanographic and Arctic data series were investigated to study possible causes of this phase reversal (Yndestad et al., 2004; Yndestad, 2007).

This presentation summarizes a number of data series analyses of North Atlantic water and the Barents Sea ecosystem. The phase relation between the temporary periodic lunar nodal cycles illustrates the chain of events between the tidal fluctuations and fluctuations in the Barents Sea ecosystem. The chain of events in the ocean system and the ecosystem is explained by resonance between the forced tidal oscillation and the coupled ocean oscillations and ecosystem oscillation. The summary concludes that there is a hidden long-term temporary deterministic process in North Atlantic water and the Barents Sea. Long-term cycles introduce phase reversals in superharmonic cycles. The deterministic property is thus dependent on the measured scale.

2. Materials and methods

2.1. The data series

The North Atlantic water data series was provided by the FRS Marine Laboratory, Aberdeen, Scotland (William Turrell, personal communication). The data were monitored within the core of the Slope Current on the Scottish side of the Faroe–Shetland Channel. The data series covers the period between 1893 and 2002 and has no values from 1895 to 1902, 1915–1922, 1930–1933, and 1941–1946. Data from these periods were cubic interpolated.

The Kola section temperature data series was provided by the Polar Research Institute of Marine Fisheries and Oceanography (PINRO), Murmansk, in Russia (Vladimir Ozhigin, personal communication). The data used here are monthly temperature values from the upper 200 m of the Kola section, along the 33°30′E medial from 70°30′N to 72°30′N in the Barents Sea (Bochkov,

1982; Tereshchenko, 1997). The temperature data series contains quarterly and annual values from the year 1900 to 2005 and monthly values from 1921 to 2005, some of which are measured and some of which are calculated. The gaps in the time series were filled by Bochkov (1982) by means of calculations using multiple regression models.

The Barents Sea zooplankton data series represents zooplankton by average biomass (dry weight, $\mathrm{g\,m^{-2}}$). The data series was provided by ICES (ICES, 2006) and covers the period 1984–2005. The Barents Sea capelin (*Mallotus villosus*) data series was provided by ICES (ICES, 2006) and covers the period 1965–2005. The data series of Northeast Arctic cod (*Gadus morhua*) covers the period 1866–2005. Data from the period 1866 to 1946 were given in Godø (2003). The data are interpolated from catch numbers to biomass by the scaling of 3.5 tons/number. The period 1946–2005 was provided by ICES (2006).

2.2. Systems theory

The investigated system is represented by the simplified general system model:

$$S(t) = \{B(t), \{S_{\mathrm{sun}}(t), S_{\mathrm{moon}}(t), S_{\mathrm{earth}}(t), S_{v}(t)\}\},$$
$$S_{\mathrm{earth}}(t) = \{B_{\mathrm{earth}}(t), \{S_{\mathrm{ocean}}(t), S_{\mathrm{atm}}(t), S_{\mathrm{eco}}(t), S_{\mathrm{ve}}(t)\}\}, \tag{1}$$

where $S_{\mathrm{sun}}(t)$ represents the sun system, $S_{\mathrm{moon}}(t)$ the moon system, $S_{\mathrm{earth}}(t)$ the earth system, $S_{v}(t)$ represents an unknown source, and $B(t)$ represents a mutually oscillating gravity force between the systems. The oscillating force $B(t)$ influences the earth system $S_{\mathrm{earth}}(t)$, which has mutual binding $B_{\mathrm{earth}}(t)$ between the $S_{\mathrm{ocean}}(t)$ ocean system, the $S_{\mathrm{atm}}(t)$ atmospheric system, the $S_{\mathrm{eco}}(t)$ ecosystem, and an unknown source $S_{\mathrm{ve}}(t)$.

2.3. The lunar nodal tide

The gravity relation $B(t)$, between the sun, the earth, and the moon, influences the cross-point between the moon plane and the ecliptic plane to the sun. This cross-point describes a *lunar nodal cycle* of 18.6134 yr. The corresponding cycle of the changing inclination of the moon's orbit with respect to the earth's equatorial plane is described by the model

$$u(t) = 23°27' + 5°09'\sin(\omega_T t + \varphi_T), \tag{2}$$

where $\omega_T = 2\pi/T = 2\pi/18.6134\,(\mathrm{rad/yr})$ is the lunar nodal angle frequency, $\varphi_T = 0.90\pi\,(\mathrm{rad})$ the lunar nodal cycle phase, and $t\,(\mathrm{yr})$ the time. The cycle amplitude has a maximum in November 1987 and a minimum in March 1996 (Pugh, 1996).

This forced lunar nodal gravity oscillation introduces a global 18.6-yr amplitude tide and a 9.3-yr phase tide in the earth ocean systems. The forced lunar nodal tide vectors have vertical and horizontal components. The vertical nodal amplitude tide is generally called Mn and has an angle frequency of $\omega_T = 2\pi/T = 2\pi/18.6134\,(\mathrm{rad/yr})$ and phase angle of $\varphi_T = 0.90\pi$. The Mn tide is a global standing wave that can be described by the function $\mathrm{Mn} = K(1-3\sin^2(\mathrm{Fi})/2\cos(L))$, where K is a constant, Fi is the earth latitude, and L the earth longitude. The standing wave has a maximum at the equator, which is twice as large as the maximum at the poles. The tide has the minimum amplitude and the maximum current at 35°N and 35°S, respectively (Mazzarella and Palumbo, 1994). The horizontal current component has an expected phase delay of about $\varphi_T(t) = (0.90-0.50)\pi\,(\mathrm{rad})$. The lunar nodal phase tide has an angle frequency of $\omega_{T/2} = 4\pi/T = 2\pi/9.3\,(\mathrm{rad/yr})$ and an angle phase of $\varphi_{T/2}(t) = 1.41\pi\,(\mathrm{rad})$ (Pugh, 1996; Boon, 2004). For a vertical sea-surface

displacement, this may be written as

$$u(t) = \sum_n a_n \sin(n\omega_T t + \varphi_n(t)) + v(t), \tag{3}$$

where a_n represents a position dependent cycle amplitude, $\omega_T = 2\pi/T$ (rad/yr) is the cycle period, and $\varphi_T(t)$ the time-dependent phase angle, which is dependent on the tide position and the position of the moon and the sun. $v(t)$ is a disturbance from an unknown source. A cycle number n may have values $n = 1, 2, 3, \ldots$ on superharmonic cycles, $n = 1/2, 1/3, \ldots$ on super-harmonic cycles for the period $t = 1800-2007$.

2.4. The coupled ocean oscillation

The vertical lunar nodal amplitude tide is about 3–4 cm. A small amplitude over a long period may, however, have a long-term influence on ocean feedback systems. This paper suggests that the analyzed long-term hydro-graphic time series indicate that tidal mixing may be an important controlling mechanism for the properties, and perhaps magnitude, of the thermohaline circulation. The thermohaline circulation may be represented by a set of feedback loops. A single feedback loop may be represented by the simple state model:

$$x(t) = a(t)x(t - \tau) + u(t) + v(t), \tag{4}$$

where $u(t)$ represents the forced oscillating lunar nodal tidal input to ocean circulation, $x(t)$ is the current state at the time t, τ the ocean circulation delay, $a(t)$ the time-dependent circulation loss, and $v(t)$ is a disturbance from an unknown source. The circulation delay τ may have resonance with the forced periodic cycles in $u(t)$. It may be shown that the forced tidal cycle $u(t)$ has resonance in the feedback system for $\omega(2n+1)\tau = \omega_T t$, and $\omega\tau = \omega_T(2n+1)t$, when $n = 0, 1, 2, 3, \ldots$ (Nayfeh and Mook, 1995). This indicates that a forced oscillating tide on a non-linear oceanographic feedback system is expected to produce dominant uneven harmonic and superharmonic cycles.

2.5. The coupled ecosystem oscillation

This paper suggests that the 18.6-yr lunar nodal amplitude tide and 9.3-yr nodal phase tide introduce a forced mean oscillating inflow to the Barents Sea. Thus, a long-term oscillating Atlantic inflow will have a long-term influence on the Barents Sea temperature, salinity, and plankton. The Barents Sea ecosystem species have a set of life cycles from recruitment to maximum spawning biomass. Each lifecycle is a feedback loop that interacts with other feedback loops. Barents Sea ecosystem dynamics may be understood as a coupled oscillation system, with the forced tidal inflow synchronized to the Barents Sea. A single biomass feedback loop may be represented by the simple model:

$$x_b(t) = a(t)x_b(t - \tau) + v(t), \tag{5}$$

where $x_b(t)$ represents the biomass recruitment at the time t, τ is the delay to maximum spawning biomass, and $a(t)$ is the time-variant recruitment rate. The recruitment rate $a(t)$ has an exponential relation $a(t) = A\exp(j\omega_T t)$ to the lunar nodal tide inflow (Yndestad, 1999). A non-linear coupled oscillation system is expected to have a resonance with the forced tidal periods $\omega(2n+1)\tau = \omega_T t$, and $\omega\tau = \omega_T(2n+1)t$, when $n = 0, 1, 2, 3, \ldots$ (Nayfeh and Mook, 1995).

For separated tidal inflow, we may expect that the 9.3-yr phase tide will optimize biomass periods of about $9.3/3 = 3.1$, 9.3, and $3 \times 9.3 = 27.9$ yr. The 18.6-yr amplitude tide will optimize biomass periods of about $18.6/3 = 6.2$, 18.6, and $3 \times 18.6 = 55.8$ yr. In this case, the 3-yr life cycle of Barents Sea capelin is expected to have fluctuation periods of about 3.1, $3 \times 3.1 = 9.3$, and

$3 \times 9.2 = 27.9$ yr. The 6-yr life cycle of Northeast Arctic cod is expected to have biomass fluctuations of about 6.2, $3 \times 6.2 = 18.6$, and 3×18.6 yr. When the 9.3-yr and the 18.6-yr tides are active at the same time, the optimum fluctuation is dependent on the phase relation between the phase tide and the amplitude tide (Yndestad and Stene, 2002; Yndestad, 2003a).

2.6. The management oscillation

The Barents Sea ecosystem oscillation is explained by a set of optimum life cycles controlled by the long-term tidal Atlantic inflow to the Barents Sea (Eq. (6)). The annual quota of landings may be 20–50% of the biomass of Northeast Arctic cod (Yndestad, 2001). This high level of landing may influence the biomass level and the long-term biomass oscillation. This problem may be easily shown when the ecosystem model (Eq. (6)) is modified by the management control law $K(t)(t-\tau_m)$ to

$$x_b(t) = a(t)x_b(t - \tau) + K(t)(t - \tau_m) + v(t), \tag{6}$$

where $K(t)$ represents the annual landings rate at the time t and τ_m represents the phase delay between biomass and the estimated biomass phase. When Barents Sea species have an optimum life cycle of about $\tau = 6-7$ yr, a dynamic phase delay in stock assessment of about $\tau_m = 3$ yr will introduce an unstable management oscillation. A second problem is that a management delay τ_m may lead to a desynchronization between the tidal Atlantic inflow and the long-term biomass fluctuation. This may lead to a biomass reduction or collapse (Yndestad, 2003a; Yndestad and Stene, 2002).

2.7. Cycle period identification

The traditional methods of spectrum analysis cannot identify cycle periods and cycle phase in time-variant stochastic processes; so, in this study, the time series have been analyzed by wavelet transformation to identify the temporary dominant cycle periods $u_n(t)$ and the time-variant phase angle $\varphi_{nT}(t)$. The periodicity was identified by a three-step investigation. The first step was to compute the wavelet spectrum by the transformation

$$W_{a,b}(t) = \frac{1}{\sqrt{a}} \int_R x(t)\Psi\left(\frac{t - b}{a}\right)dt, \tag{7}$$

where $x(t)$ is the analyzed time series and $\Psi(\cdot)$ is a coiflet wavelet impulse function (Daubechies, 1992; Matlab, 1997). $W_{a,b}(t)$ is a set of wavelet cycles, b is the translation in time, and a is the time-scaling parameter in wavelet transformation. The relationship between wavelet scaling (a) and the sinus period T is about $T \approx 1.2a$. In this analysis, the translation is $b = 0$, thus, the computed wavelet transformation $W_a(t)$ represents a moving correlation between $x(t)$ and the impulse function $\Psi(\cdot)$ over the whole time series $x(t)$. Using this wavelet transformation, it is possible to identify single, long-period cycles in a short time series. Errors at the beginning and at the end of a time series are reduced in the following manner. The time series are scaled in amplitude and to the zero mean value by the scaling transformation $y(t) = [x(t)-\text{mean}(x(t))]/\text{var}(x(t))$, where $x(t)$ is the time series, and $y(t)$ is the scaled time series. Subsequently, the time series is expanded with symmetric values at the beginning and end of the time series.

The cycle period of single dominant-wavelet cycle is identified by computing the autocorrelation for the wavelet spectrum $R_w(\tau) = E[W_a(t)W_a(t+\tau)]$. Dominant, stationary wavelet cycles have maximum values in the autocorrelation functions. Periodic cycles in the autocorrelation function of the wavelet spectrum demonstrate that there is a stationary cycle. The cycle period

phase is identified by the optimum correlation between dominant wavelets and lunar nodal cycles by $R_{nT}(\tau) = E[W_{an}(t)u_{nT}(t)]$, where $u_{nT}(t)$ is an nT lunar nodal cycle period and the phase angle $\varphi_{nT}(t)$ is a free variable. The correlation quality is computed by the Pearson correlation coefficient $Q_{nT} = R\,\mathrm{sqr}[(k-2)/(1-R^2)] \sim t(k-2)$, where R is the correlation coefficient and k the number of samples. Q_{nT} is tested against a t-distribution by $(k-2)$ numbers of freedom to determine whether the correlation is statistically significant (von Storch and Zwiers, 1999).

2.8. Temperature and biomass forecast

The temperature and biomass forecasts are based on a set of 1-yr predictions developed with the model

$$x(t+1) = f\left(\sum_n w_n, x_n(t), u_n(t)\right), \qquad (8)$$

where $x(t)$ represents the data series, $x(t+1)$, a 1-yr predicted data series, w_n, weights in a trained neural network, and $u(t)$ the deterministic lunar nodal cycle spectrum of 74.4, 55.8, 18.5, 9.3, and 3.1 yr, where each amplitude was scaled to 1.0. In this analysis, the forecast was based on a trained neural network (Masters, 1995; NeuralTools, 2005). The network was trained on 80% of the data series and tested on the remaining 20%.

3. Results

3.1. Ocean oscillations

3.1.1. The lunar nodal tides

The 18.6-yr lunar nodal amplitude tide is related to the forced lunar nodal gravity cycle, which has a stationary phase angle of about 0.90π (rad). This period may then serve as a phase reference in the data series analysis. A number of data series of the annual mean sea level of Aberdeen and Murmansk have been investigated by analyzing the wavelets spectrum. All data series had dominant cycles related to the 18.6-yr amplitude tide (Yndestad et al., 2004). The Aberdeen data series wavelet spectrum had an optimum correlation $R = 0.88$ to the 18.6-yr lunar nodal amplitude cycle at the phase angle $(0.90–0.10)\pi$ (rad). This estimate represents a phase delay of about 0.10π (rad) for about 0.9 yr. The annual mean Murmansk sea level had an optimum correlation $R = 0.70$ for the 18.6-yr lunar nodal cycle at the phase angle $(0.90–0.20)\pi$ (rad) or a phase delay of about 1.8 yr. The annual mean sea level at the Norwegian coastline had a dominant 18-yr cycle for the phase angle $(0.90–0.10)\pi$ (rad) from Bergen to Rørvik and about $(0.90–0.20)\pi$ (rad) from Rørvik to Vardø.

The 9.3-yr phase tide was identified for the annual mean sea level at Aberdeen and Murmansk. At Aberdeen, the dominant 9-yr cycle had a correlation $R = 0.39$ for the 9.3-yr phase tide at the phase angle $(1.41–0.50)\pi$ (rad). The correlation between the 9-yr wavelet and the 9.3-yr tide was $R = 0.8$ at Murmansk by the phase angle $(1.41–0.90)\pi$ (rad). This indicates a phase delay between Aberdeen and Murmansk of about 0.40π (rad) or 2 yr.

The sea level at Stockholm has been monitored since 1774 and represents the longest sea-level data series in the world (Ekman, 2003). A wavelet analysis of this data series has a correlation $R = 0.55$ and $Q = 10$ with a 74.4-yr superharmonic lunar nodal cycle at the phase angle 0.75π (rad). Identification of the 74-yr superharmonic cycle indicates that there are longer superharmonic periodic cycles in North Atlantic water. The identified phase thus serves as a reference in the analysis of other data series.

3.1.2. North Atlantic water temperature

Fig. 1 shows the North Atlantic water temperature in the Faroe–Scotland Channel between 1900 and 2005, the predicted temperature from 2005 to 2020, the estimated 74-yr tide cycle, the identified dominant 18-yr wavelet cycle, and the 18.6-yr tide cycle. The data series shows that there was a cold period from about 1900 to 1925, a warm period from about 1925 to 1970, and another cold period until about 1990, after which a new warm period began.

The North Atlantic water temperature fluctuations are related to the sum of the 18.6-yr lunar nodal amplitude tide, 9.3-yr lunar nodal phase tide, and a superharmonic tide of about $18.6 \times 4 = 74.4$ yr. The legged correlations with the lunar nodal tide cycles are estimated to be $R = 0.59$ for the phase tide and $R = 0.68$ and $R = 0.93$ for the amplitude tide (Yndestad et al., 2004; Yndestad, 2006). The tidal properties have a temporary deterministic property, which opens the possibility of predicting expected future temperature fluctuations. The mean temperature fluctuation has a correlation $R = 0.93$ with the 74.4-yr superharmonic cycle at the phase angle $(0.75–0.46)\pi$ (rad). A phase delay of 0.46π (rad) behind the 74-yr sea-level tide indicates that the long-term 74-yr fluctuation is associated with the current aspect of North Atlantic water fluctuation.

The lunar nodal spectrum has information about expected variability in the data series. To predict expected future states, data history information and the future lunar nodal spectrum must be combined. The temperature fluctuation from 2005 to 2020 was forecast by a trained Multi-Layer Feedforward Network (Masters, 1995; NeuralTools, 2005). Dependent input for the network was the temperature data series and lunar nodal spectrum; 20% of the testing data had 1.01 root mean square error and a 0.64 absolute standard deviation error. The predicted fluctuations indicate that we may expect a cold period before the average temperature continues to increase until about 2020. We may expect maximum warm periods from about 2000 to 2008 and after about 2016, when the tidal cycles of 74.4, 18.6, and 9.3 are simultaneously positive. These estimates indicate that the warm climate fluctuation from 1990 has about the same deterministic fluctuation properties as those identified from about 1925.
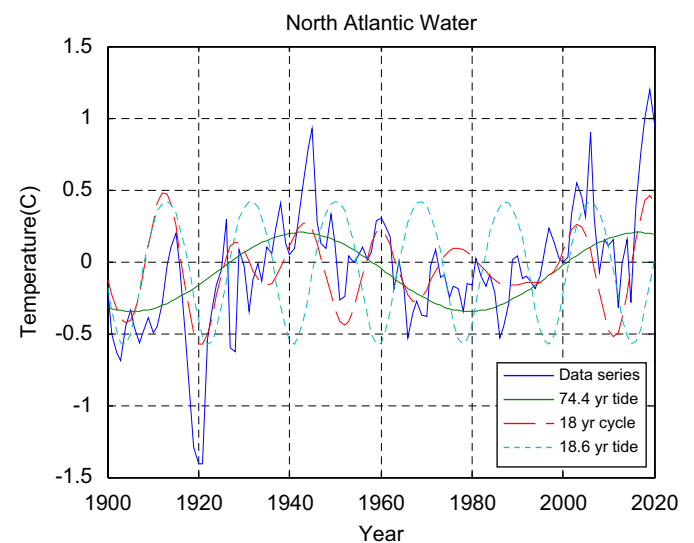

Fig. 1. North Atlantic water temperature from 1900 to 2005 and temperature predictions from 2005 to 2020. The estimated 74.4-yr tide cycle, the identified 18-yr wavelet cycle, and the 18.6-yr tide cycle are also shown. The 74.4- and 18.6-yr tide references have scaled amplitudes on the figure to demonstrate the phase relation to the tidal estimates.

3.1.3. The Kola section water temperature

Fig. 2 shows the annual mean Kola section temperature series, the astronomic 18.6-yr tide cycle, the identified dominant 18-yr wavelet cycle, and the identified 74.4-yr superharmonic tide cycle. The 74.4-yr tide cycle follows the average mean fluctuations in the data series from 1900 and explains why the temperature had a maximum at about 1940 and why the annual mean temperature has continued to increase since 1980. The identified 18-yr cycle has a phase delay of about 0.25π (rad) related to the astronomic 0.9π (rad) lunar nodal phase angle. This delay shows that the dominant 18-yr temperature fluctuation is related to the current aspect of warm Atlantic inflow to the Barents Sea. The relationship between the 18-yr wavelet cycles and the nodal tide cycles shows that the 18-yr cycle phase may have a phase reversal when the 74.4-yr tide changes from a negative to a positive state.

Table 1 presents a summary of the identified dominant lunar nodal cycles in North Atlantic water and the Barents Sea. The 74.4-yr tidal reference is estimated from a 74-yr cycle in the extent of Arctic ice (Yndestad, 2006). The amplitude tide has

a northward phase delay of about 0.10π (rad) or 0.9 yr to Aberdeen and a 0.30π (rad) or 1.8-yr delay to Murmansk. The 9.3-yr phase tide has a northward phase delay of about 0.50π (rad) or 2.3 yr to Aberdeen and 0.90π (rad) or 4.2 yr to Murmansk. The estimated dominant 18 cycles in the Kola region have reversed phase angles in accordance with the estimated lunar nodal amplitude tide from 1925. In North Atlantic water, the estimated deviation is only 0.10π (rad) or less than a year. The estimated dominant 9-yr cycle temperature cycles have a phase error of only 0.20π (rad) in the Kola section and 0.15π (rad) in North Atlantic water.

The wavelet analysis shows that the dominant 18-yr cycle in North Atlantic water and in the Kola section had a 1.0π (rad) phase reversal at about 1925. The physical explanation of this phase reversal is a 18.6-yr amplitude tide and 18-yr temperature fluctuations that start to fluctuate in the opposite direction.

3.2. Barents Sea ecosystem oscillation

3.2.1. The Barents Sea zooplankton biomass

Fig. 3 shows the Barents Sea zooplankton dry weight biomass data series from 1984 to 2005, the predicted biomass for 2005–2020, the 18.6-yr lunar nodal tide cycle, and the 9.3-yr lunar nodal phase tide cycle. For the period 1984–2005, the biomass increased from about $2\,\mathrm{g\,m^{-2}}$ in 1984 to about $13\,\mathrm{g\,m^{-2}}$ in 1994. The predictions from 2005 to 2020 are based on a trained multi-layer feed-forward network (Masters, 1995; NeuralTools, 2005). Dependent input for the network was the data series and lunar cycles of 18.6 and 9.3 yr. The estimated error for 22 test data samples was 0.65 root mean square error and a 0.60 standard deviation of absolute error. The predicted forecast has a warm period from about 2000 to 2008 and a new warm period after about 2016.

The zooplankton biomass fluctuations are related to the inverse 18.6- and 9.3-yr tidal cycles. The biomass reached a minimum at about 1990, when the astronomic lunar nodal tide cycles were simultaneously positive, and reached a maximum in 1994, when they were negative. The correlations between the zooplankton data series and the 18.6- and 9.3-yr lunar nodal tide cycles are estimated to be $R = -0.5$ in the period 1984–2005. The zooplankton biomass has a life cycle of about 1 yr. The biomass dynamics are then expected to follow the long-term Atlantic Current inflow to the Barents Sea.
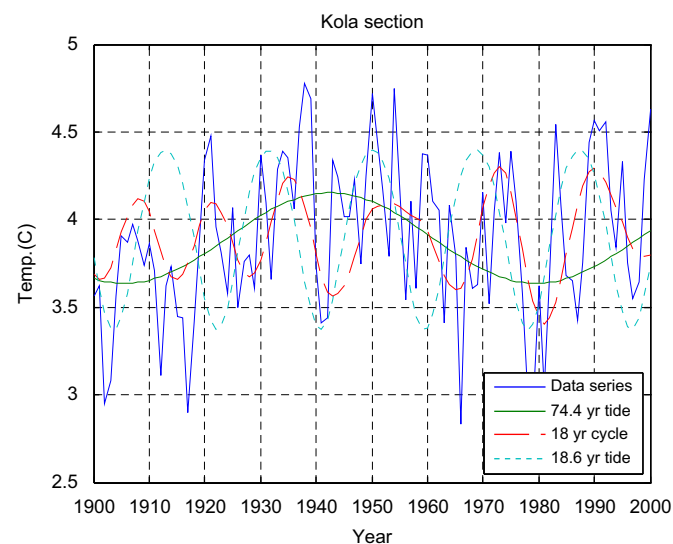

Fig. 2. Temperature series from 1900 to 2000, the 18.6-yr tide, the 74.4-yr tide, and the identified 18-yr cycle are shown for the Kola section of the Barents Sea. The 18.6-yr tide reference has a scaled amplitude on the figure to demonstrate the phase relation to the lunar nodal tide.

Table 1
Identified dominant lunar nodal cycles in North Atlantic water and the Barents Sea.

Time series	Time (yr)	Nodal cycle ω_0 (rad/yr)	Cycle phase ϕ (rad)	Phase reversals -1.0π (rad)	Correlation R	Correlation quality Q
Tide reference						
74.4-yr tide		$2\pi/74.4$	0.75π			
18.6-yr tide		$2\pi/18.6$	0.90π			
9.3-yr tide		$2\pi/9.3$	1.41π			
Faroe−Shetland						
Aberdeen Sea level	1952–2003	$2\pi/18.6$	$(0.90-0.10)\pi$		0.88	42
Aberdeen Sea level	1952–2003	$2\pi/9.3$	$(1.41-0.50)\pi$		0.39	3.1
NAW temp.	1895–2004	$2\pi/74.4$	$(0.75-0.56)\pi$		0.93	27.8
NAW temp.	1895–2004	$2\pi/18.6$	$(0.90-0.0/0.85)\pi$	1925	0.68	8.3
NAW temp.	1895–2004	$2\pi/9.3$	$(1.41-0.65)\pi$		0.59	4.7
Barents Sea						
Murmansk Sea level	1952–2003	$2\pi/18.6$	$(0.90-0.20)\pi$		0.70	7.0
Murmansk Sea level	1952–2003	$2\pi/9.3$	$(1.41-0.90)\pi$		0.80	9.3
Kola temp.	1900–2005	$2\pi/74.4$	$(0.75-0.41)\pi$		0.95	32.6
Kola temp.	1900–2005	$2\pi/18.6$	$(0.90-1.2/0.2)\pi$	1925	0.77	10.0
Kola temp.	1920–2005	$2\pi/9.3$	$(1.41-1.00)\pi$	1960	0.74	6.9

3.2.2. The Barents Sea capelin oscillation

Fig. 4 shows the Barents Sea capelin biomass between 1972 and 2005, the astronomic 18.6-yr amplitude tide, and the 9.3-yr phase tide cycle. The biomass prediction for 2005–2015 is based on a trained generalized regression neural net (Masters, 1995; NeuralTools, 2005). Dependent input for the network was the Stock data series, the Maturing data series, the Recruit data series, and lunar cycles of 18.6, 9.3, and 3.1 yr. The estimated error for 20% of the test data was 1667 root mean square error and a 1176 standard deviation for the absolute error.

The figure shows that the biomass has fluctuations related to the 9.3-yr lunar nodal tidal periods. The biomass life cycle time of about 3 yr introduces a phase delay between the tidal oscillation and the biomass oscillation. Two life cycle periods of 3 yr caused peaks in biomass at about 1975 and 1980. In the period between 1980 and 1985, the recruitment rate was minimal and there were biomass collapses when the 18.6-yr and the 9.3-yr tides became negative. From 1985 to 1990, the recruitment rate increased due to tidal inflow. The 9.3-yr tide synchronized capelin recruitment and the biomass increased to a new maximum level. After, 1992 the tidal cycles became negative. There was no new growth period and, after the 3-yr life cycle period, there was another biomass collapse. A new growth period occurred from about 1997 to 2000, when the 9.3-yr tidal inflow turned positive. In this instance, it was a small growth period since the 18.6-yr tide was negative.

The predicted biomass for 2005–2015 suggested that we can expect a new biomass growth period from 2006 to 2010, when the 9.3-yr tide is positive. The biomass collapses between the maximum 9.3-yr tidal inflows indicate that biomass growth is not related to a linearly increasing temperature, but rather to synchronization between the 9-yr Atlantic tidal inflow to the Barents Sea and 3-yr capelin biomass life cycle dynamics.

3.2.3. The Northeast Arctic cod oscillation

Fig. 5 shows the data series of Northeast Arctic cod biomass from 1866 to 2005, the astronomic 18.6-yr tide cycle, dominant 18-yr wavelet cycle, and superharmonic 55.8-yr cycle. The biomass of Northeast Arctic cod has an optimum life cycle period of about 6–7 yr (Yndestad, 1999) and Fig. 5 demonstrates the long-term biomass fluctuation well. The dominant 18-yr wavelet cycle
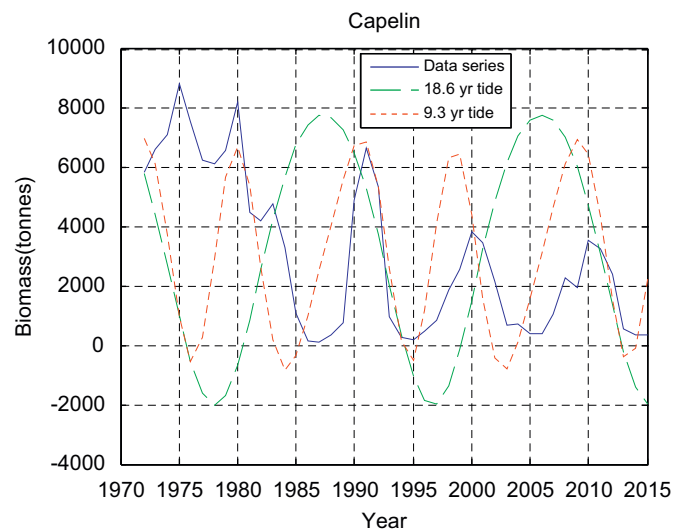

Fig. 4. Barents Sea capelin biomass from 1972 to 2005, with the biomass prediction for 2005 to 2015, the astronomic 18.6-yr tide cycle, and the 9.3-yr tide cycle. The 18.6- and the 9.3-yr tide are scaled on the figure to demonstrate the phase relation to the lunar nodal tide.
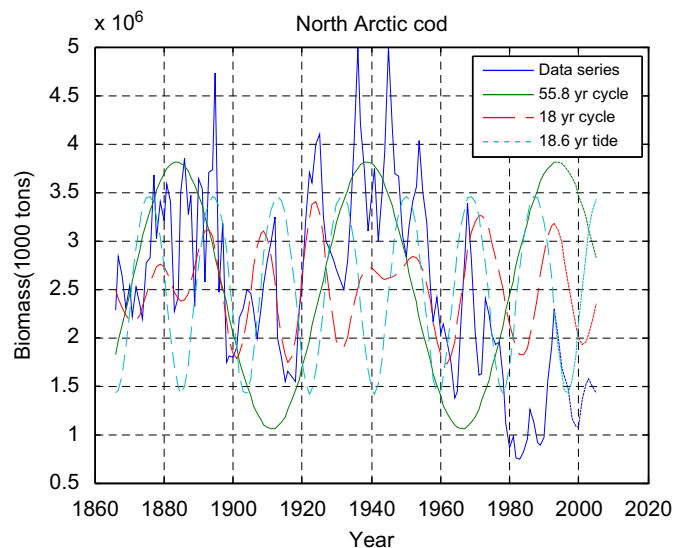

Fig. 5. Data series of Northeast Arctic cod biomass from 1866 to 2005, the astronomic 18.6-yr tide cycle, dominant 18-yr wavelet cycle, and superharmonic 55.8-yr cycle. The 55.8-yr and 18.6-yr periods are scaled on the figure to demonstrate the phase relation to the biomass fluctuation.
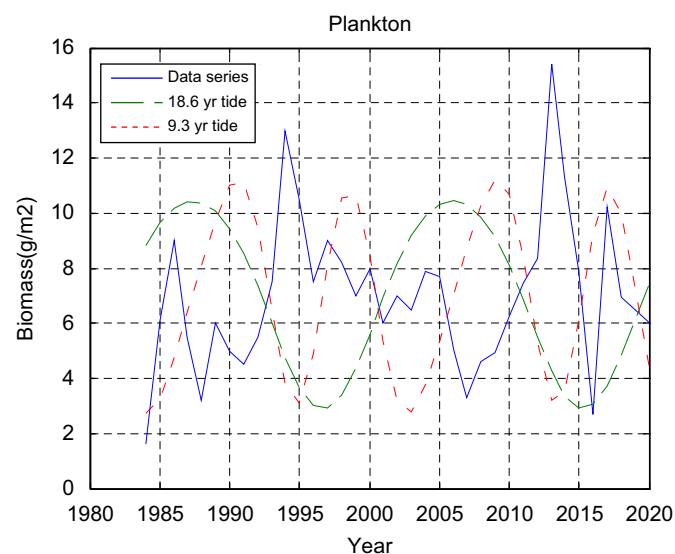
has a phase delay with the 18.6-yr amplitude tide. Analysis of North Atlantic water temperature and Kola section temperature shows that the 18-yr temperature had a phase reversal of 1.0π (rad) at about 1922. This phase reversal explains why the 18-yr wavelet cycle has a phase angle before the 18.6-yr tide until 1920. The presented $3 \times 18.6 = 55.8$-yr cycle in Fig. 5 demonstrates the relationship between the cycle and the long-term biomass fluctuation from 1860 to 1980, when there was a strong biomass caused by over-fishing. The correlation of the identified dominant 55-yr cycle is estimated to be $R = 0.65$ for the entire data series.

Wavelet spectrum analysis of data series from species in the Barents Sea ecosystem has identified dominant cycle periods correlated with the lunar nodal spectrum (Yndestad, 2003a, b). Table 2 shows the biomass life cycle period, the identified dominant fluctuation periods in rad/yr, the cycle phase angle,

Fig. 3. Barents Sea zooplankton dry weight biomass data series from 1984 to 2005 is shown, along with the biomass prediction for 2005 to 2020, the astronomic 18.6-yr amplitude tide, and the 9.3-yr phase tide. The 9.3-yr tide is scaled on the figure to demonstrate the phase relation to the lunar nodal tide.

Table 2
Barents Sea biomasses and their life cycles, dominant fluctuations, and correlations with the lunar nodal spectrum.

Data series	Life cycle (yr)	Dominant cycle (rad/yr)	Cycle phase (rad)	Correlation R
Murmansk tide				
18.6-yr tide		$2\pi/18.6$	0.70π	
9.3-yr tide		$2\pi/9.3$	0.51π	
Ecosystem				
Zooplankton	1	$2\pi/18.6$	$(0.70-0.05)\pi$	-0.50
Zooplankton	1	$2\pi/9.3$	$(0.51+0.50)\pi$	
Capelin	3	$2\pi/18.6_T$	$(0.70-0.15)\pi$	0.73
Capelin	3	$2\pi/9.3$	$(0.51-0.42)\pi$	0.73
Shrimp	6–7	$2\pi/18.6$	$(0.70+0.85)\pi$	0.85
Shrimp	6–7	$2\pi/6.2$	$-0.09/-1.09\pi$	
Herring	6–7	$2\pi/55.8$	0.90π	0.92
Herring	6–7	$2\pi/18.6$	$(0.70+0.35)\pi$	
Herring	6–7	$2\pi/6.2$	$-0.09/-1.09\pi$	
Cod	6–7	$2\pi/55.8$	0.86π	0.65
Cod	6–7	$2\pi/18.6$	$(0.70-0.48)\pi$	
Cod	6–7	$2\pi/6.2$	$-0.09/-1.09\pi$	
Haddock	6–7	$2\pi/18.6$	$(0.70-0.48)\pi$	
Haddock	6–7	$2\pi/6.2$	$-0.09/-1.09\pi$	

and the correlation between the dominant-wavelet cycle and the lunar nodal inflow to the Barents Sea. In this analysis, the phase is related to the identified lunar nodal cycle in the data series of Murmansk sea level. The table shows that the biomass of all of the investigated species in the Barents Sea ecosystem have dominant fluctuations related to the lunar nodal tides.

The phase relation between the tidal inflow and the biomass fluctuation illustrates the chain of events in the Barents Sea ecosystem. The Barents Sea zooplankton biomass has a 1-yr life cycle. The 9.3-yr biomass fluctuation has a phase relation of $+0.50\pi$ (rad/yr) before the 9.3-yr tide. This means that the zooplankton growth is correlated with the current aspect of less 9.3-yr Atlantic tidal inflow to the Barents Sea. The 18-yr fluctuation has a negative correlation between the biomass and the 18.6-yr amplitude tide.

The Barents Sea capelin biomass has an optimum life cycle of about 9.3/3 or 3 yr (Yndestad and Stene, 2002). The dominant 9-yr fluctuation has an estimated phase delay of -0.42π (rad/yr) or 2 yr from the maximum 9.3-yr tide. The estimated phase delay between the plankton fluctuation and the capelin fluctuation is estimated to be $(0.50+0.42)\pi = 0.92\pi$ (rad/yr) or 4.2 yr. A 0.92π (rad/yr) delay between zooplankton oscillation and capelin oscillation shows that the capelin biomass growth has a positive direction as long as zooplankton biomass fluctuation is increasing.

The Barents Sea shrimp biomass has a life cycle of about 18.6/3 or 6–7 yr. The dominant 18-yr fluctuation has an estimated phase relation of $+0.85\pi$ (rad/yr) or 7.9 yr before the 18.6-yr tide reference. This phase has a current relationship with growth and an 18.6-yr tidal inflow. The shrimp biomass has growth when the 18.6-yr tidal inflow is positive.

The Norwegian spring spawning herring biomass has a life cycle of about 18.6/3 or 6–7 yr. In this biomass, the dominant 18-yr fluctuation has an estimated phase relation of $+0.35\pi$ (rad/yr) or 3.2 yr before the 18.6-yr tide reference. The long-term fluctuation is estimated to be about 50–60 or $3 \times 18.6 = 55.8$ yr. The Northeast Arctic cod biomass has the same life cycle period, about 18.6/3 or 6–7 yr. The dominant 18-yr fluctuation in the cod biomass data series has an estimated phase relation of -0.48π (rad/yr) or 4.5 yr after the 18.6-yr tide reference. The phase relation between the 18-yr herring and cod fluctuations is about $(0.35+0.48)\pi$ (rad/yr) or 7.7 yr. This relation indicates that the

biomass fluctuations of herring and cod are related to the biomass fluctuations of zooplankton and capelin at different age levels (Yndestad and Stene, 2002). The Northeast Arctic haddock biomass has about the same biomass oscillations as the biomass of Northeast Arctic cod.

The biomass of shrimp, capelin, herring, cod, and haddock have optimum life cycles of about 6–7 yr. This life cycle period was reflected as a dominant 6-yr wavelet cycle. The identified 6-yr cycles have the same phase angle and phase reversal. The phase reversal is most likely caused by interference when the 6-yr life cycle interacts with the 18.6-yr and 9.3-yr tide inflows.

3.3. The management oscillation

The Barents Sea ecosystem is optimized by synchronization between the ocean oscillation and the biomass feedback oscillation. An oscillation biomass will influence the quota of landings and thus introduce a management oscillation. Historical records indicate that there is a phase delay (Eq. (6)) between the age structure in cod biomass assessment and in biomass landings. A 3-yr phase delay will introduce a reversed phase between the 6-yr biomass fluctuation and management fluctuation and will introduce an unstable biomass fluctuation (Yndestad, 2001).

Long-term biomass growth is dependent on a close phase relation between the long-term biomass fluctuation and the long-term landing fluctuations. Historical records of Northeast Arctic cod show a mismatch between biomass growth and landings during the period 1945–1985. In this period, landings increased and the 18- and 55-yr cycles were turning in a negative direction. The biomass of Norwegian spring spawning herring was reduced in the same period and collapsed in the 1960s, when the 18.6- and 9.3-yr tides were turning in a negative direction (Yndestad, 2001). This case illustrates the importance of synchronization between the long-term biomass oscillation and the management oscillation.

Synchronization between the ecosystem oscillation and the management oscillation requires control of the management oscillation phase. This is a well-known problem from control theory that may be solved by feed-forward control. However, feed-forward control requires a good estimate of future fluctuations. This future estimate may be based on a trained neural network, as demonstrated in Figs. 1, 3, and 4.

4. Discussion

4.1. The forced nodal tide oscillation

Analysis of the annual mean sea-level data series from Aberdeen to Murmansk identified the 18.6-yr amplitude tide in all data series (Yndestad et al., 2004). This was an expected observation and is well known from many other observations (Boon, 2004). The unexpected observations are the phase delay between Aberdeen and Murmansk, identification of the 9.3-yr phase tide, and identification of the long-term 74-yr tidal fluctuation. A possible explanation of the phase delay is more shallow water at the coastline between Rørvik and Murmansk. More shallow water will influence the relationship between the tidal vertical amplitude and the tidal horizontal current. The 9.3-yr phase delay of about 0.5π (rad) indicates a current-driven fluctuation. The annual sea level at Stockholm (Ekman, 2003) represents the longest sea-level data series in the world. The wavelet analysis identified, most likely for the first time, a dominant 74-yr superharmonic tidal cycle in this data series. The cause of the fluctuation is unclear. A possible explanation is

that energy from the lunar nodal tides is distributed in the ocean circulation system.

4.2. The methods

The analysis is based on high-quality data series. The wavelet analysis method has been used to identify single fluctuations and phase in time-variant data series. The close relationship between the known lunar nodal cycle and the identified dominant cycles confirms that the wavelet analysis is a robust method to identify cycle periods and phase in data series. At the same time, the wavelet method has limitations at the start and end of the data series. The identified long 74-yr periods then need to be compared with similar identifications in other data series.

4.3. The coupled ocean temperature oscillation

The wavelet analysis of the North Atlantic water data series identified 18- and 9-yr dominant temperature fluctuations that correlated in terms of cycle time and phase with the 18.6-yr amplitude tide and the 9.3-yr phase tide. The fluctuating mean value correlated with a 74-yr superharmonic cycle. The same dominant periods were identified in the Kola section temperature data series, delayed by about 2 yr. Sutton and Hudson (2005) analyzed Atlantic Multidecadal Oscillation (AMO) from 1871 to 2003 and found a possible relationship with the ocean's thermohaline circulation. The present analysis suggests that the North Atlantic temperature fluctuation is influenced by vertical and horizontal lunar nodal harmonic tides.

The wavelet analysis of the oceanographic data series shows that there is no linear relationship between the lunar nodal tides and the temperature fluctuations. The 18-yr temperature cycle in North Atlantic water and in the Barents Sea has phase reversals at about 1925. The mechanism behind this phase reversal is unclear. The wavelet data series analysis shows that the phase reversal is associated with the 74-yr superharmonic cycle that controls fluctuation of the mean Atlantic water temperature. This period is identified in a number of long data series. Records from the periods of 3150 BC to 2400 BC and 622 AD to 1470 AD show a peak with periods of 18.4, 53, and 77 yr. Greenland ice cores show periodic cycles of 20, 78, and 181 yr and temperature records from central England from 1700 to 1950 show periodicities at cycles of 23 and 76 yr (Borroughs, 1992; Schlesinger and Ramankutty, 1994; Currie, 1995). A possible source that produces this periodic cycle is a 74-yr circulation of Arctic water in the Arctic Ocean (Bonisch and Schlosser, 1995; Yndestad, 2006).

4.4. Phase reversals

The wavelet analysis of the oceanographic data series shows that there is no linear relationship between the 18.6-yr amplitude tide and the identified 18-yr temperature fluctuations. The 18-yr temperature cycle in North Atlantic water and in the Barents Sea had phase reversals at about 1925. Phase reversals are well known in physical and communication systems. In relation to the 18.6-yr tide, a phase reversal was identified by Currie (1987, 1995) in long Nile records, and Mazzarella and Palumbo (1994) in atmospheric pressure and the NAO winter index (Yndestad, 2006).

The physical mechanism behind this phase reversal is unclear. Phase reversals can arise in forced oscillating non-linear systems (Stoker, 1950; Magnus, 1965). This investigation shows that the phase reversal is associated with the 74-yr superharmonic cycle. A possible explanation is interference between the forced lunar nodal tides and non-linear feedback system in the Atlantic or Arctic Ocean. When a forced stationary 18.6-yr cycle $u_T(t) = a_T(t)\sin(\omega_T t)$ accumulates in an oscillating 74-yr superharmonic cycle $u_{4T}(t) = a_{4T}(t)\sin(\omega_{4T} t)$, the 74-yr superharmonic cycle $u_{4T}(t)$ will introduce a phase reversal when $a_{kT}(t) \gg a_T(t)$ and $u_{4T}(t)$ has a shift between the positive and negative states.

4.5. The Barents Sea ecosystem oscillation

The Barents Sea ecosystem analysis shows that the biomass life cycle and the long-term fluctuations are correlated with the lunar nodal tide spectrum (Table 2). Barents Sea capelin has a life cycle that is related to a third harmonic of the 9.3-yr tide. The life cycles of shrimp, cod, herring, and haddock were related to a third harmonic of the 18.6-yr tide. The biomass growth was synchronized with the lunar nodal tide. The biomass growths of zooplankton and shrimp had reversed phases. The long-term biomass fluctuations of cod and herring were correlated with a cycle period of about $3 \times 18.6 = 55.8$ yr.

This analysis suggests that we may understand the Barents Sea ecosystem dynamic as a free-coupled oscillating system of forced lunar nodal tides. A free-coupled oscillating system is expected to have optimum third harmonic and third superharmonic oscillations (Strogatz and Stewart, 1993; Nayfeh and Mook, 1995). This mechanism is similar to resonance in physics. When Northeast Arctic cod biomass has an optimum life cycle of about 6–7 yr, the fluctuation amplitude and phase are expected to be related to the 18.6-yr tidal inflow to the Barents Sea. The 18.6-yr biomass has an optimum long-term fluctuation of 3×18.6 or about 55 yr. Barents Sea capelin has an optimum life cycle of about 3 yr. The fluctuation amplitude and phase are expected to be related to the 9.3-yr tidal inflow to the Barents Sea. The identified phase reversals in North Atlantic water inflow indicate that we may understand this as a temporary coupled system.

The physical explanation of ecosystem oscillation as a small tidal oscillating Atlantic inflow to the Barents Sea has a powerful influence when it is integrated in time and space, in the same direction. The long-term mean inflow thus influences zooplankton production, biomass recruitment, and biomass growth in the food chain. In a very long period of tidal inflow, biomass life cycle periods are optimized by the periods of tidal inflow. The biomass grows in periods when the amplitude tide and the phase tide grow. The biomass declines when the tides decline. If the quota of landing grows in periods when the biomass declines, there is a risk for biomass collapse. This observation supports a previous theory from Hjort (1914), as well as many later observations, that biomass growth is dependent on matching of recruitment and zooplankton fluctuation.

Understanding the ecosystem as a coupled oscillating system implies that the biomass is a temporarily stable oscillating system. The synchronization between the ocean oscillation and the management oscillation influences long-term biomass growth. The long-term biomass growth of cod and herring started after the ocean temperature phase reversal at about 1922 when there was a special tidal event. The current biomass state of cod and herring is a result of management from the 1960s to 1980. The current biomass state of capelin biomass is a result of management in the 1980s. This demonstrates that long-term biomass growth is dependent on a set of optimum recruitment life cycles.

5. Conclusion

The present investigation has identified long lunar nodal tides as a hidden source that has a temporary deterministic influence on the temperature fluctuation in North Atlantic water and the Barents Sea ecosystem. The explanation is that a small tide may have a major influence on the ocean's thermohaline circulation

system and the Barents Sea ecosystem, when the tides are integrated in time and space over a long period. The results suggest that we may understand the long-term ocean variability as an oscillation system coupled to the forced 9.3-yr phase tide and the 18.6-yr amplitude tide. The tidal influence on the circulating water introduces tide-related temperature fluctuations in North Atlantic water. This temperature fluctuation has a phase reversal associated with a 74-yr superharmonic cycle.

All investigated species in the Barents Sea ecosystem have optimum life cycles related to 9.3- and 18.6-yr tidal inflows to the Barents Sea. We may then understand the Barents Sea ecosystem as a free non-linear oscillating system coupled to the lunar tidal inflow to the Barents Sea. The ecosystem has adapted optimum biomass fluctuations related to third harmonics and the third superharmonic of the Atlantic tidal inflow to the Barents Sea. The Barents Sea capelin fluctuation is associated with harmonics from the 9.3-yr phase tide. Northeast Arctic cod, Barents Sea shrimp, Norwegian spring spawning herring, and Barents Sea haddock fluctuations are associated with harmonics from the 18.6-yr lunar nodal amplitude tidal inflow to the Barents Sea.

References

Bochkov, Yu.A., 1982. Water temperature in the 0–200 m layer in the Kola-Meridian section in the Barents Sea, 1900–1981. Sbornik Nauchnykh Trudov 46, 113–122 (in Russian).

Bonisch, G., Schlosser, P., 1995. Deep water formation and exchange rates in the Greenland/Norwegian Seas and the Eurasian Basin of the Arctic Ocean derived from tracer balances. Progress in Oceanography 35, 29–52.

Boon, J.D., 2004. Secrets of the Tide. Horwood Publishing.

Borroughs, W.J., 1992. Weather Cycles Real or Imaginary? Cambridge University Press, Cambridge.

Currie, R.G., 1987. Examples and implications of 18.6- and 11-yr terms in world weather records. In: Rampino, M.R., Sanders, J.E., Newman, W.S., Konigsson, L.-K. (Eds.), Climate: History, Periodicity, and Predictability. International Symposium held at Barnard College, Columbia University, New York, 21–23 May 1984 (R.W. Fairbridge Festschrift) Van Nostrand Reinhold, New York, NY, pp. 378–403, 588pp. (Chapter 22).

Currie, R.G., 1995. Variance contribution of M_n and S_c Signals to Nile River Data over a 30-8 year bandwidth. Journal of Coastal Research Special Issue No. 17: Holocene Cycles: Climate, Sea Levels and Sedimentation, pp. 29–38.

Currie, R.G., Wyatt, T., O'Brie, D.P., 1993. Deterministic signals in European fish catches, wine harvests, sea level, and further experiments. International Journal of Climatology 8, 255–281.

Darwin, G.H., 1880. On the secular change of the orbit of a satellite revolving about a tidally distorted planet. Philosophical Transactions of the Royal Society of London 171, 713–891.

Daubechies, I., 1992. Ten lectures of wavelet. SIAM Journal on Mathematical Analysis 24, 499–519.

Ekman, M., 2003. The World's Longest Sea Level Series and a Winter Oscillation Index for Northern Europe 1774–2000. Small Publications in Historical Geophysics. No. 12. Summer Institute for Historical Geophysics Åland Islands.

Ellertsen, B., Fossum, P., Sundby, S., 1989. Relation between temperature and survival of eggs and first feed in larvae of northeast Arctic cod (*Gadus morhua* L.). Rapports et Procès-verbaux des Réunions du Conseil international pour l'Exploration de la Mer 191, 209–219.

Godø, O.R., 2003. Fluctuation in stock properties of north-east Arctic cod related to long-term environmental changes. Fish and Fisheries 4, 121–137.

Helland-Hansen, B., Nansen, F., 1909. The Norwegian Sea. Fiskeridirektoratets skrifter. Havundersøkelser 2, 1–360.

Hjort, J., 1914. Fluctuations in the Great Fisheries of Northern Europe. Andr. Fred. Høst and Files, Copenhagen, April.

Hylen, A. 2002. Fluctuations in abundance of Northeast Arctic cod during the 20th century. ICES Marine Science Symposia 215, 543–550.

ICES, 2006. Report of the Arctic Fisheries Working Group (AFWG). ICES CM 2006/ACFM:25, ICES Headquarters, 19–28 April 2006.

Keeling, C.D., Whorf, T.P., 1997. Possible forcing global temperature by oceanic tides. Proceedings of the National Academy of Sciences of the United States of America 94, 8321–8328.

Lindquist, A., 2002. Herring periods of Bohuslan: a cross-sectorial approach. ICES Marine Science Symposia 215, 343–351.

Ljungman, A.V., 1879. Bidrag till løsningen af frågan om de stora sillfiskenas sekulära periodisitet. Tidskrift for Fiskeri 5, 257–268 (in Swedish).

Magnus, K., 1965. Vibrations. Blackie, London.

Maksimov, I.V., Sleptsov-Shevlevich, B.A., 1970. Long-term changes in the tide-generation force of the moon and the iciness of the Arctic Seas. Proceedings of the N.M. Knipovich Polar Scientific-Research and Planning Institute of Marine Fisheries and Oceanography (PINRO) 27, 22–40.

Maksimov, I.V., Smirnov, N.P., 1964. Long-range forecasting of secular changes of the general ice formation of the Barents Sea by the harmonic component method. Murmansk Polar Science Research Institute, Sea Fisheries 4, 75–87.

Maksimov, I.V., Smirnov, N.P., 1965. A contribution to the study of causes of long-period variations in the activity of the Gulf Stream. Oceanology 5, 15–24.

Maksimov, I.V., Smirnov, N.P., 1967. A long-term circumpolar tide and its significance for the circulation of ocean and atmosphere. Oceanology 7, 173–178 (English edition).

Masters, T., 1995. Advanced Algorithms for Neural Network. Wiley, New York.

Matlab, 1997. Matlab. Wavelet Toolbox. User's Guide. The Math Works Inc.

Mazzarella, A., Palumbo, A., 1994. The lunar induced-signal in climatic and oceanic data over the Western Mediterranean Area and on its bistable phaing. Theoretical and Applied Climatology 50, 93–102.

Nakken, O., 1994. Causes of trends and fluctuations in the Arco-Norwegian cod stock. ICES Marine Science Symposium 198, 212–228.

Nayfeh, A.H., Mook, D.T., 1995. Nonlinear Oscillators. Wiley, New York.

NeuralTools, 2005. Neural Tools Sophisticated Neural Network for Spreadsheets. Version 1.0, November, 2005. Palisade Corporation, USA.

Petterson, O., 1905. On the probable occurrence in the Atlantic Current of variations periodical, and otherwise, and their bearing on metrological and biological phenomena. Rapport et Procès-verbaux des Réunions du Conseil international pour l'Exploration de la Mer 42, 221–240.

Pettersson, O., 1915. Long periodical (sic) variations of the tide-generating force. Conseil Permanente International pour l'Exploration de la Mer (Copenhagen), Pub. Circ. No. 65, pp. 2–23.

Pettersson, O., 1930. The tidal force. A study in geophysics. Geografiska Annaler 18, 261–322.

Pugh, D.T., 1996. Tides, Surges and Mean Sea-Level. Wiley, New York.

Royer, T.C., 1993. High-latitude oceanic variability associated with the 18.6-year nodal tide. Journal of Geophysical Research 98, 4639–4644.

Schlesinger, M.E., Ramankutty, N., 1994. An oscillation in the global climate system of period 65–70 years. Nature 367, 723–726.

Stoker, J.J., 1950. Non-Linear Vibrations in Mechanical and Electrical Systems. Interscience, New York.

von Storch, H., Zwiers, F.W., 1999. Statistical Analysis in Climate Research. Cambridge University Press, Cambridge.

Strogatz, S.H., Stewart, I., 1993. Coupled oscillators and biological synchronization. Scientific American 269, 102–109.

Sutton, R.T., Hudson, D.L.R., 2005. Atlantic Ocean forcing North American and European summer climate. Science 309, 115–117.

Sætersdal, K., Loeng, H., 1987. Ecological adaption of reproduction in Northeast Arctic cod. Fishery Research 5, 253–270.

Tereshchenko, V.V., 1997. Seasonal and Year-to-Year Variation in Temperature and Salinity of the Main Currents along the Kola Section in the Barents Sea. PINRO Publ., Murmansk, 71pp. (in Russian).

Wegner, G., 1996. Herring research: remarks on a 250-year-old theory. ICES Information. 28:8.

Wyatt, T., Currie, R.G., Saborido-Ray, F., 1994. Deterministic signals in Norwegian cod records. ICES Marine Science Symposium 198, 49–55.

Yndestad, H., 1999. Earth nutation influence on system dynamics of Northeast Arctic cod. ICES Journal of Marine Science 56, 652–657.

Yndestad, H., 2001. Earth nutation influence on Northeast Arctic management. ICES Journal of Marine Science 58, 799–805.

Yndestad, H., 2003a. The code of long-term biomass cycles in the Barents Sea. ICES Journal of Marine Science 60, 1251–1264.

Yndestad, H., 2003b. The cause of biomass dynamics in the Barents Sea. Journal of Marine Systems 44, 107–124.

Yndestad, H., 2006. The Lunar nodal cycle influence on Arctic climate. Journal of Marine Science 63, 401–420.

Yndestad, H., 2007. The Arctic Ocean as a coupled oscillating system to the forced 18.6 yr lunar nodal cycle. In: Tsonis, Anastasios A., Elsner, James B. (Eds.), Advances in Nonlinear Geosciences. Springer, New York.

Yndestad, H., Stene, A., 2002. Systems dynamics of Barents Sea Capelin. ICES Journal of Marine Science 59, 1155–1166.

Yndestad, H., Turrell, W.R., Ozhigin, V., 2004. Temporal linkages between the Faro-Shetland time series and the Kola section time series. ICES Annual Science conference in Vigo, September 2004. Theme Session M. Regime Shifts in the North Atlantic Ocean: Coherent or Chaotic?